Journal of Applied Polymer Science

Theoretical and experimental investigations of the inverse emulsion polymerization of acrylamide

Ardeshir Abdi, Mohammad Shahrokhi, Ahmad Ramazani S. A., Ehsan Vafa
Department of Chemical and Petroleum Engineering, Sharif University of Technology, P. O. Box 11155-9645, Tehran, Iran
Correspondence to: M. Shahrokhi (E-mail: shahrokhi@sharif.edu)

ABSTRACT: In this study, the inverse emulsion polymerization modeling of polyacrylamide with population balance equations (PBEs) was performed. The PBEs were derived on the basis of the zero–one kinetic model. The effects of the surfactant steric barrier and surfactant reaction with radicals, including monomeric radicals, on the radical entry rate into the particle were taken into account. In the modified model, the coagulation phenomenon was included through consideration of the effects of forces not included in the Derjaguin, Landau, Verwey, and Overbeek (DLVO) theory; these include hydration and steric forces in addition to DLVO forces. The effects of the surfactant and initiator concentrations on the conversion, particle size, and average molecular weight (MW) were investigated by simulation and experimental studies. Increasing the surfactant concentration initially increased the conversion and decreased MW. A further increase in the surfactant concentration resulted in a decrease in the conversion and an increase in MW. The average particle size decreased with an increase in the surfactant concentration. An increase in the initiator concentration led to an increase in the monomer conversion and a decrease in the average MW. © 2015 Wiley Periodicals, Inc. J. Appl. Polym. Sci. **2015**, *132*, 41916.

KEYWORDS: coagulation; inverse emulsion polymerization; modeling; polyacrylamide; population balance equation; steric barrier

Received 25 March 2014; accepted 1 January 2015
DOI: 10.1002/app.41916

INTRODUCTION

Water-soluble polymers are an important class of materials because of their numerous applications. Polymers based on polyacrylamide (PAM) and its derivatives are widely used as commercial polymers, particularly in wastewater treatment applications, enhanced oil recovery, paper making, and drug delivery. In some applications, such as enhanced oil recovery, nanopolymers with a high molecular weight (MW) is required.[1] Water-in-oil emulsion polymerization (EP) is one of the ideal methods for obtaining such polymers.[2,3]

The kinetic mechanism of inverse emulsion polymerization (IEP) can be affected by many factors, including the types of initiator and surfactant and the rate of mixing. Research studies have been conducted since the 1960s to investigate the mechanism and kinetics of IEP.[4] Later studies on the IEP of acrylamide showed that the mechanisms of nucleation depend on the type and solubility of the initiator in the aqueous or oil phase and the concentration of the surfactant.[5,6]

IEP is not a mirror image of an ideal EP,[7] but there are similarities in some aspects. Most kinetic studies over the years have focused on batch EP, and several studies have been reported in the literature. Two alternative models in the population balance format, namely the zero–one and pseudo-bulk models, are widely used for modeling conventional EP.[8,9] These studies have helped to elucidate the various competing mechanisms involved and have led to a number of mathematical models (with different degrees of complexity) that are able to estimate the key product attributes.[9,10] Nevertheless, the attempts to model IEP have been few, and some aspects of this process in these studies have been ignored. The first proposed model for IEP was developed by Hunkeler *et al.*[11] They considered the IEP model to be equal to inverse microsuspension polymerization, in which the drop nucleation is the only mechanism for particle formation, and the homogeneous and micellar nucleations were ignored. Alexander *et al.*[12] proposed a model for the IEP of PAM based on the Monte Carlo method. According to their result, the number of free radicals per particle was 0.5, whereas later studies showed that this parameter was less than 0.5.[13] Through experimental study, Capek[13] showed that the rate of entry and exit of radicals into and out of the particle in IEP were less than the predicted values obtained by the relations used for EP modeling.

In an IEP reaction system, particle nucleation, the evolution of the particle size distribution (PSD), and other final product properties are strongly related to the type of surfactant and its concentration. According to relevant investigations,[11,13] electrosteric surfactants, such as sorbitan monooleate (Span 80), have a steric barrier for radical entry into and exit from the particle.

Moreover, this surfactant (based on the structure of its molecules) can react with the radicals, and this can lead to the termination or transfer of the radical to the surfactant.[11,14,15] Therefore, these phenomena will affect the entry and exit rates of the radicals into and out of the particles. Thickett and Gilbert[16] modified the rate of radical entry into the particle for propagation-controlled entry for the reaction of the steric surfactant poly(acrylic acid) in the EP of styrene.

Another phenomenon in IEP is coagulation between the polymer particles, which significantly influences the final properties of the product. Many attempts have been made to develop mathematical models for describing coagulation between polymer particles.[9,17] General approaches have been based on the theory developed by Derjaguin, Landau, Verwey, and Overbeek (DLVO), which provides a quantitative measure of the attractive van der Waal's and electrostatic repulsive forces between two particles. Additional interactive forces, such as long-range dispersion forces and short-range hydration forces, are known to be important for electronegative atoms bonded to hydrogen atoms and structural forces because of the concentration of water molecules in hydration shells.[18,19] However, unlike DLVO forces, non-DLVO forces are very difficult to either measure experimentally or predict theoretically, particularly in the case of complex colloidal systems. Moreover, hydration forces can be different in different systems,[19] and the model developed for a specific colloidal system is often difficult to apply to other systems. In the IEP of PAM, the PAM molecule contains highly electronegative atoms, such as oxygen and nitrogen, in its chemical amine group. Therefore, hydration forces created by the interaction between water molecules and the electronegative atoms of PAM should be considered in the modeling of the coagulation phenomenon.

As stated before, a comprehensive model that can predict the PSD in the IEP by taking into account the coagulation phenomenon, steric barrier effect of the electrosteric surfactant, and surfactant reactions has not been previously reported in the literature. In this study, such a model was proposed for modeling the IEP of acrylamide in a batch reactor to predict the PSD of PAM on basis of the zero–one model. The effects of the steric barrier and the reactions of the surfactant with oligomeric radicals are considered in the calculation of the average MW of the polymer. The proposed model was validated through experimental studies.

EXPERIMENTAL

Materials

To purify the acrylamide crystals (purity $\geq$ 99%, analytical grade, Fluka Co.), we dissolved them in methanol and recrystallized them again. 2,2-Azoisobutyronitrile (AIBN) as an oil-soluble initiator was purified in the same manner with ethanol as a solvent. The surfactant used in this study was Span 80 (sorbitan monooleate). The deionized water and *n*-hexane were used as the aqueous and oil phases, respectively.

Polymerization

The polymerization reaction was carried out in a batch reactor at temperature of 60°C. Polymerization was performed in a glassy batch reactor with volume of 500 mL, and the temperature inside the reactor was controlled at 60°C through manipulation of the reactor jacket temperature. To perform the reaction, 280 mL of *n*-hexane containing 0.44 g of the nonionic surfactant Span 80 was added to the reactor. An amount of 25 g of the acrylamide monomer dissolved in 130 mL of deionized water was injected to the reactor. To start the reaction, 0.02 g of the oil-soluble initiator AIBN dissolved in 10 mL of *n*-hexane was charged into the reactor. The polymerization was performed for 150 min at 60°C with stirring at a rate of 600 rpm.

In all of the experiments, during the material injection and reaction times, the reactor was under a blanket and purge of nitrogen.

Measurements of the Particle Size, MW, and Conversion

During the reaction time, samples were taken to measure the reaction conversion, average MW, and PSD. The reaction conversion was determined according to the procedure described in Barari *et al.*[5] To determine the conversion of acrylamide during the reaction time, samples with a volume of 10 mL [with a mass of m_1 (g)] were taken from the reactor at various time intervals. To stop the polymerization reaction in the sample, 1 mL of an aqueous solution of hydroquinone (1.5 wt %) was added to each sample. Then, the PAM was precipitated with an excess amount of acetone, and the obtained precipitate was separated and dried *in vacuo* at 50°C. The obtained white product was washed with acetone several times again to remove traces of acrylamide in the final product and to purify the PAM. The remaining solid was dried *in vacuo* for 24 h until a constant weight was obtained (m_2; g). The conversion of acrylamide was calculated as follows:

$$\%\text{Conversion} = \frac{\acute{m}_2}{(m_1 x)} \times 100 \quad (1)$$

where $\acute{m}_2$ is the corrected weight of the dried polymer powder (with the amount of hydroquinone added to the samples subtracted) and x is the weight ratio of the initial monomer relative to all of the materials used in the polymerization.

The average MW was determined by the measurement of the viscosity of the solution obtained by solving the produced PAM in water at different concentrations and using the correlation between the viscosity and average MW.[20] To obtain the PSD, the scanning electron microscopy (SEM) technique was used. For this purpose, first a sample was taken from the reactor, and the reaction was stopped by the addition of hydroquinone to the sample. To prevent particle aggregation, the sample was diluted with extra solvent (hexane), and additional surfactant was added to the sample. A few drops of the diluted solution were placed on the sample holder and then freeze-dried *in vacuo*. We obtained the particle morphology and size distribution by taking images from the sample using the SEM technique.[5]

As a sample, the SEM results of the final product are shown in Figure 1.

MODELING OF IEP

When the initiator is soluble in the oil phase, IEP is the mirror image of EP, and EP modeling can be extended for IEP modeling.[21] The initiator used in this study (AIBN) for the inverse polymerization of AM was soluble in the oil phase, and

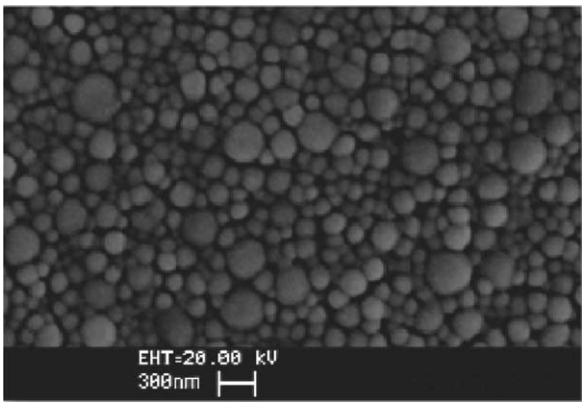

Figure 1. SEM result for the final PAM product.

therefore, EP modeling could be used. The zero–one model has been successfully adopted to describe free-radical polymerization in confined systems, especially EP, where the entry of a radical into a particle containing a radical leads to instantaneous termination. As stated by Gilbert,[9] the conditions required for a system to obey zero–one kinetics are $\rho/c \ll 1$ and $k/c \ll 1$, where ρ is the first-order rate coefficient for radical entry, k is the exit rate of a radical from the particle, and c is the mutual annihilation of two radicals. Gilbert also showed that the condition for the applicability of zero–one kinetics that is both sufficient and necessary is $C^{SL} \gg k_p C_p$, where C^{SL} is the pseudo-first-order rate coefficient for termination between a short chain and a long chain, k_p is the propagation rate coefficient, and C_p is the monomer concentration in the growing particle. For the system under consideration, the previous conditions were satisfied except for very large particles (>200 nm), and therefore, the zero–one kinetic model was selected.[9,10] Under these circumstances, the zero–one kinetic model with some modifications could be used to model the IEP of AM in batch reactors. In this study, we used the zero–one model by taking into account the surfactant steric barrier and its reactions with radicals for the modeling of IEP. In this section, first, the IEP reactions were described, and then, the mass balances were determined for all components. Next, the population balance on the basis of the zero–one model was used to obtain the PSD. Finally, the equation for obtaining the average MW was determined.

IEP Reactions

IEP was initiated in the oil phase by the decomposition of the oil-soluble initiator (AIBN) and the production of the primary radical (R_{io}), which propagated with monomer molecules to produce oligomeric radicals. The kinetic reactions in IEP like conventional EP include initiation, propagation, nucleation, radical entry into the particle, radical desorption from the particle, termination, and chain transfer. As mentioned in the previous section, electrosteric surfactants, such as Span 80, can participate in the termination and chain-transfer reactions. As shown in Figure 2, this surfactant contains an active double bond. It has five labile hydroxyl groups that can participate in chain-transfer reactions. The double bond in the chemical structure of the Span 80 molecule can react with oligomeric radicals, and this leads to termination.[11,22] The concentrations of active hydrogen bonds (AHB) and active double bonds (ADB) of the surfactant are shown by [AHB] and [ADB], respectively. The reaction kinetics are presented in Table I.

In Table I, SP refers to the polymer produced by the reaction of the surfactant by oligomeric radicals. If SP is produced by the reaction of ADB of the surfactant molecule with the oligomeric radical, the produced polymer does not have double bonds and is denoted by SP′. On the other hand, if the reaction is carried out by AHB of the surfactant molecule, SP has an active double bond in the middle tail of the surfactant molecule (denoted by SP″) and has the potential to participate in the polymerization again. The fact that in the particle phase the AHBs are more accessible than the ADB leads to an increase in the probability of transfer relative to termination by ADB.[22]

Mass Balances for the Initiator, Oligomers, Monomer, and Surfactant

The mass balances for the initiator and oligomers are given by the following equations:

$$\frac{d([I]V_{oil})}{dt} = -k_i[I]V_{oil} \tag{2}$$

$$\frac{d([R_{io}]V_{oil})}{dt} = \left(2f_{in}k_i[I] - k_d[R_{io}][M_o] - k_t[R_{io}]\sum_{i=0}^{j_{cr}-1}[P_o^i] - k_{t,[ADB]}[ADB_o][R_{io}] - k_{tr,[AHB]}[AHB_o][R_{io}] - k_{t,[AHB]}\sum_{j=0}^{j_{cr}-1}[(AHB-jM)_o^*]\ [R_{io}]\right)V_{oil} \tag{3}$$

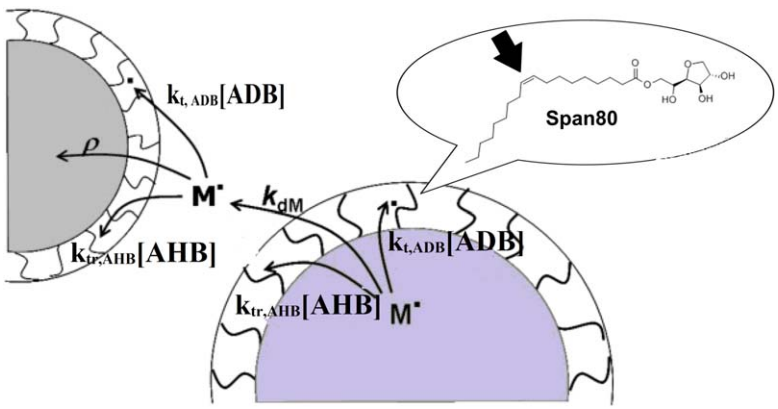

Figure 2. Reactions of the exiting and entry radicals with an electrosteric surfactant.[23] [Color figure can be viewed in the online issue, which is available at wileyonlinelibrary.com.]

Table I. Reaction Scheme

Oil-phase reactions	
Initiator decomposition	$I \xrightarrow{k_i} 2R_{io}$
Initiation	$R_{io} + M_o \xrightarrow{k_d} P_o^1$
Propagation	$P_o^i + M_o \xrightarrow{k_p} P_o^{i+1} \quad i=0,1,2,\cdots,j_{cr}-1$
Chain transfer to monomer	$P_o^i + M_o \xrightarrow{k_{tr,M}} DP + P_o^0 \quad i=1,2,\cdots,j_{cr}-1$
Termination	$P_o^i + P_o^j \xrightarrow{k_t} DP,$
Radical entry into the particle	$P_o^i + Particle \xrightarrow{\rho_{init}} R_i \ , \quad i=z,z+1,\ldots,j_{cr}-1,$
Monomeric radical entry into the particle	$P_o^0 + Particle \xrightarrow{\rho_I^E} E$
Radical entry into the hairy layer	$P_o^i + Particle \xrightarrow{\rho_{init}^0} P_{HL}^i$
Monomeric radical entry into the hairy layer	$P_o^0 + Particle \xrightarrow{\rho_0^E} E_{HL}$
Homogeneous nucleation in the oil phase	$P_o^{j_{cr}-1} + M_o \xrightarrow{k_p} P_o^{j_{cr}}(particle)$
Chain transfer to the surfactant in the oil phase	$P_o^i + \mathrm{AHB}_o \xrightarrow{k_{tr,[AHB]}} DP + \mathrm{AHB}_o^*$
Propagation by AHB of the surfactant	$\begin{cases} \mathrm{AHB}_o^* + M_o \xrightarrow{k_{[AHB]}^p} (\mathrm{AHB}-M)_o^* \\ (\mathrm{AHB}-jM)_o^* + M_o \xrightarrow{k_{[AHB]}^p} \left(\mathrm{AHB}-(j+1)M\right)_o^* \end{cases}$
Termination by ADB of the surfactant	$\begin{cases} \mathrm{ADB}_o + \mathrm{P}_o^i \xrightarrow{k_{t,[ADB]}} SP', \quad i=1,2,\ldots,j_{cr}-1 \\ \mathrm{ADB}_o + R_{io} \xrightarrow{k_{t,[ADB]}} IP \end{cases}$
Termination for the AHB radicals of the surfactant	$\begin{cases} (\mathrm{AHB}-jM)_o^* + \mathrm{P}_o^j \xrightarrow{k_{t,[AHB]}} SP'' \\ (\mathrm{AHB}-jM)_o^* + R_{io} \xrightarrow{k_{t,[AHB]}} IP \end{cases}$
Particle-phase reactions	
Propagation	$R_i + M_p \xrightarrow{k_p} R_{i+1} \quad i=0,1,2,\ldots$
Chain transfer to monomer	$R_i + M_p \xrightarrow{k_{tr,M}} DP + E$
Termination	$R_i + \mathrm{R_j} \xrightarrow{k_t} DP$
Desorption of the monomeric radical from the particle phase into the oil phase	$f_1^M \xrightarrow{k_{dM,HL}(r)} P_o^0 + f_0$
Desorption of the monomeric radical into the hairy layer	$f_1^M \xrightarrow{k_{dM}} f_0 + E_{HL}$
Surfactant-layer reactions around the particles (hairy layer)	
Chain transfer to the surfactant for the entry radical	$\mathrm{P}_{HL}^i + \mathrm{AHB}_{HL} \xrightarrow{k_{tr,[AHB]}} DP + \mathrm{AHB}_{HL}^*$
Propagation by AHB of the surfactant	$\begin{cases} AHB_{HL}^* + M_{HL} \xrightarrow{k_{[AHB]}^p} [\mathrm{AHB}-\mathrm{M}]^*_{\mathrm{HL}} \\ (\mathrm{AHB}-iM)_{HL}^* + M_{HL} \xrightarrow{k_{[AHB]}^p} \left(\mathrm{AHB}-(i+1)M\right)_{HL}^* \end{cases}$

Table I. *Continued*

Termination for the AHB radicals of the surfactant	$(\mathrm{AHB}-jM)^{*}_{HL}+\mathrm{P}^{\mathrm{i}}_{\mathrm{HL}} \xrightarrow{k_{t,[AHB]}} \mathrm{SP}$, $\mathrm{i}=z, z+1, \ldots, \mathrm{j}_{cr}-1, j=0,1,2,\ldots,\mathrm{j}_{\sigma}-1$
Termination of the monomeric radical by AHB	$(\mathrm{AHB}-jM)^{*}_{HL}+E_{HL} \xrightarrow{k_{t,[AHB]}} \mathrm{SP}$
Termination of the radicals by ADB	$\mathrm{P}^{\mathrm{i}}_{\mathrm{HL}}+\mathrm{ADB}_{HL} \xrightarrow{k_{t,[ADB]}} \mathrm{SP}'$
Termination of the monomeric radical by ADB	$E_{HL}+\mathrm{ADB}_{HL} \xrightarrow{k_{t,[ADB]}} \mathrm{SP}'$

$$\frac{d([P_o^1]V_{\mathrm{oil}})}{dt}=\Big(k_d[R_{\mathrm{io}}][M_o]+k_p[M_o][P_o^0] -(k_p+k_{\mathrm{tr},M})[P_o^1][M_o]-k_t[P_o^1][T] -k_{t,[\mathrm{ADB}]}[\mathrm{ADB}_o][P_o^1]-k_{\mathrm{tr},[\mathrm{AHB}]}[\mathrm{AHB}_o][P_o^1] -k_{t,[\mathrm{AHB}]}\sum_{j=0}^{j_{cr}-1}[(\mathrm{AHB}-jM)_o^{*}]\ [P_o^1]\Big)V_{\mathrm{oil}} \tag{4}$$

$$\frac{d([P_o^n]V_{\mathrm{oil}})}{dt}=\Big((k_p[P_o^{n-1}]-k_p[P_o^n])[M_o]-k_t[P_o^n][T] -k_{\mathrm{tr},M}[P_o^n][M_o]-\mathrm{k}_{\mathrm{t},[\mathrm{ADB}]}[\mathrm{ADB}_o][P_o^n]-\mathrm{k}_{\mathrm{tr},[\mathrm{AHB}]}[\mathrm{AHB}_o][P_o^n] -k_{t,[\mathrm{AHB}]}\sum_{j=0}^{j_{cr}-1}[(\mathrm{AHB}-jM)_o^{*}]\ [P_o^n]\Big)V_{\mathrm{oil}}\ \ n=2,3,\ldots,z-1 \tag{5}$$

$$\frac{d([P_o^n]V_{\mathrm{oil}})}{dt}=\Big((k_p[P_o^{n-1}]-k_p[P_o^n])[M_o]-k_t[P_o^n][T]-k_{\mathrm{tr},M}[P_o^n][M_o] -\mathrm{k}_{\mathrm{t},[\mathrm{ADB}]}[\mathrm{ADB}_o][P_o^n]-\mathrm{k}_{\mathrm{tr},[\mathrm{AHB}]}[\mathrm{AHB}_o][P_o^n]-k_{t,[\mathrm{AHB}]} \sum_{j=0}^{j_{cr}-1}[(\mathrm{AHB}-jM)_o^{*}]\ [P_o^n]\ \Big)V_{\mathrm{oil}}-\rho^n_{\mathrm{init}}C_{Micelle}V_{\mathrm{oil}} -V_{\mathrm{oil}}\int_{r_{\mathrm{nuc}}}^{r_{\max}}\rho^n_{\mathrm{init}}f(r,t)dr\ \ n=z,z+1,\ldots,j_{cr}-1 \tag{6}$$

$$\frac{d([P_o^0]V_{\mathrm{oil}})}{dt}=\Big(k_{\mathrm{tr},M}\Big(\sum_{i=1}^{j_{cr}-1}[P_o^i]\Big)[M_o]-k_p[M_o][P_o^0] -\rho_0^E[P_o^0]C_{Micelle}-k_t[P_o^0][T]-\mathrm{k}_{\mathrm{t},[\mathrm{ADB}]}[\mathrm{ADB}_o][P_o^0] -k_{t,[\mathrm{AHB}]}\sum_{j=0}^{j_{cr}-1}[(\mathrm{AHB}-jM)_o^{*}]\ [P_o^0]\ \Big) V_{\mathrm{oil}}+V_{\mathrm{oil}}\int_{r_{\mathrm{nuc}}}^{r_{\max}}k_{dM,\mathrm{HL}}(r)f_1^M(r,t)dr -V_{\mathrm{oil}}\int_{r_{\mathrm{nuc}}}^{r_{\max}}\rho_0^E(r)f(r,t)dr \tag{7}$$

where $P_o^{\,n}$ is the concentration of oligomeric radical with the length of n and $P_o^{\,0}$ is the concentration of monomeric radical in the oil phase. In eqs. (3)–(7), k_t is termination rate coefficient between oligomeric radicals, $k_{t,[\mathrm{ADB}]}$ and $k_{t,[\mathrm{AHB}]}$ are termination rate coefficients between oligomers and the ADB and AHB radicals of surfactant, respectively, and $[(\mathrm{AHB\text{-}jM})_o{}^{*}]$ is the concentration of surfactant radicals with j monomer length in the oil phase.

Because the volume of the hairy layer around the particles is small compare to particle radius, the amount of monomer in this phase will be sufficiently low.[23] Consequently, to obtain the monomer concentrations in other phases, the partition coefficient can be used.[11,12]

The monomer concentration in the polymer particle phase ($[\mathrm{M_p}]$) is equal to its saturation concentration[12] as long as the monomer exists in droplets, and the monomer concentrations in the other phases ($[\mathrm{M_o}]$, $[\mathrm{M_d}]$ and $[\mathrm{M_{HL}}]$ are monomer concentration in the oil, droplet and hairy layer phases, respectively) can be obtained as follows:[24]

$$[M_p]=[M_p]^{\mathrm{sat}} \tag{8}$$

$$[M_o]=K_{po}[M_p] \tag{9}$$

$$[M_{\mathrm{HL}}]=\frac{[M_p]+[M_o]}{2} \tag{10}$$

$$[M_d]=\frac{M-[M_p]V_p^s-[M_o]V_{\mathrm{oil}}-V_{\mathrm{HL}}[M_{\mathrm{HL}}]}{V_d} \tag{11}$$

where K_{po} is the coefficient of monomer partitioning between polymer particles and oil phase. V_d, V_{oil} and $\mathrm{V}_p^{\,s}$ are total volume of the droplets , volume of the oil phase and total volume of swollen particles phase, respectively. When droplets are depleted from the monomer ($[M_d]=0$), the concentration of the monomer in the different phases can be obtained with eqs. (9)–(11).

The total moles of free surfactant in the oil phase (S_{oil}) is obtained by the following surfactant balance equation:[9,17]

$$S_T=S_{\mathrm{oil}}+S_a+S_d \tag{12}$$

where S_T, S_a and S_d denote the total moles of surfactant, the moles of surfactant in the hairy layer, and the moles of surfactant surrounding the droplets, respectively.

One molecule of Span 80 has one ADB and five AHB (at $t=0$, $[\mathrm{ADB}_o]V_{\mathrm{oil}}=S_{\mathrm{oil}}=S_{\mathrm{oil}}$, $[\mathrm{AHB}_o]V_{\mathrm{oil}}=5S_{\mathrm{oil}}$). Therefore, we have

$$\frac{d([\mathrm{ADB}_o]V_{\mathrm{oil}})}{dt}=-\mathrm{k}_{\mathrm{t},[\mathrm{ADB}]}[\mathrm{ADB}_o][\mathrm{T}]V_{\mathrm{oil}}+a^{\mathrm{oil}}_{\mathrm{ADB}}\frac{dS_{\mathrm{oil}}}{dt} \tag{13}$$

$$\frac{d([\mathrm{AHB}_o]V_{\mathrm{oil}})}{dt}=-\mathrm{k}_{\mathrm{tr},[\mathrm{AHB}]}[\mathrm{AHB}_o]\Big(\sum_{\mathrm{i}=1}^{\mathrm{j}_{cr}-1}[\mathrm{P}^{\mathrm{i}}_{\mathrm{o}}]+[\mathrm{R_{io}}]\Big)V_{\mathrm{oil}} +5\ a^{\mathrm{oil}}_{\mathrm{AHB}}\frac{dS_{\mathrm{oil}}}{dt} \tag{14}$$

where $a^{\mathrm{oil}}_{\mathrm{ADB}}$ and $a^{\mathrm{oil}}_{\mathrm{AHB}}$ denote the ratios of unreacted ADB of the surfactant molecules to the total ADB of the surfactant molecules and unreacted AHB of the surfactant molecules to the

total AHBs of the surfactant molecules in the oil phase, respectively.

In eqs. (13) and (14), the first term is related to the reaction of the surfactant in the oil phase, and the second term is related to the transfer of the surfactant molecules between the oil and other phases.

Because of the high activity of the P_o^0 radical, transfer to the surfactant did not occur.

It is worth mentioning that because of the steric barrier among the surfactant molecules, the reactions between the surfactant radicals are neglected. Because it is assumed that a monolayer of surfactant is formed around each particle, the fraction of particle surface that is covered by the surfactant molecules is equal to

$$\theta = \frac{K_{ad}[S_{oil}]}{1 + K_{ad}[S_{oil}]} \tag{15}$$

where $[S_{oil}]$ denotes concentration of surfactant in the oil phase and K_{ad} is Langmuir adsorption constant.[11,17] Therefore, the total moles of surfactant in the hairy layer around the total particles is given by

$$S_a = \frac{A_p}{a_s N_{av}}\theta \tag{16}$$

where N_{av} is Avogadro's number (mol^{-1}) and A_p is the total area of particles and is given by

$$A_p = V_{oil} N_{av} \int_{r_{nuc}}^{r_{max}} 4\pi r^2 f(r,t)\,dr \tag{17}$$

The moles of surfactant surrounding the droplets is obtained from the following equation:

$$S_d = \frac{V_d}{a_{ed} N_{av} r_d} \tag{18}$$

where a_{ed} and r_d are the area occupied by a single molecule of surfactant around the droplet and the average radius of droplet in the system, respectively.

The mass balances for the ADB and AHB in the hairy layer, similar to eqs. (13) and (14), can be determined as follows:

$$\frac{d([ADB_{HL}]V_{HL})}{dt} = -\left(k_{t,[ADB]}[ADB_{HL}]\left(\sum_{i=z}^{j_{cr}-1}[P^i_{HL}]\right) - k_{t,[ADB]}[ADB_{HL}][E_{HL}]\right)V_{HL} + a^{HL}_{ADB}\frac{dS_a}{dt} \tag{19}$$

$$\frac{d([AHB_{HL}]V_{HL})}{dt} = -k_{tr,[AHB]}[AHB_{HL}]\left(\sum_{i=z}^{j_{cr}-1}[P^i_{HL}]\right)V_{HL} + 5\ a^{HL}_{AHB}\frac{dS_a}{dt} \tag{20}$$

where a^{HL}_{ADB} and a^{HL}_{AHB} denote the ratios of the unreacted ADB of the surfactant molecules to the total ADB of the surfactant molecules and the unreacted AHB of the surfactant molecules to the total AHB of the surfactant molecules in the hairy layer, respectively. Moreover, $[E_{HL}]$ and $[P_{HL}{}^i]$ are the concentrations of monomeric radicals and oligomers with chain length i in the hairy layer phase, respectively.

The mass balances for the produced radicals in the hairy layer are given by

$$\begin{aligned}\frac{d([P^i_{HL}]V_{HL})}{dt} = {} & V_{oil}\int_{r_{nuc}}^{r_{max}}\rho^0_{init} f(r,t)\,dr + k_p[M_{HL}]([P^{i-1}_{HL}] \\ & - [P^i_{HL}])V_{HL} - k_{tr,[AHB]}[AHB_{HL}][P^i_{HL}]V_{HL} \\ & - k_{t,[AHB]}\sum_{j=0}^{j_{cr}-1}[(AHB-jM)^*_{HL}]\ \ [P^i_{HL}]V_{HL} \\ & - k_{t,[ADB]}[ADB_{HL}][P^i_{HL}]V_{HL} \\ & - V_{oil}\int_{r_{nuc}}^{r_{max}}\rho^i_{init} f(r,t)\,dr - k_t[P^i_{HL}]([E_{HL}] \\ & + \sum_{i=z}^{jcr-1}[P^i_{HL}])V_{HL}, \quad i = z, z+1, \ldots, j_{cr}-1\end{aligned} \tag{21}$$

$$\begin{aligned}\frac{d([E_{HL}]V_{HL})}{dt} = {} & V_{oil}\int_{r_{nuc}}^{r_{max}}\rho^E_0 f(r,t)\,dr + V_{oil}\int_{r_{nuc}}^{r_{max}} k_{dM} f(r,t)\,dr \\ & - k_{t,[AHB]}\sum_{j=0}^{j_{cr}-1}[(AHB-jM)^*_{HL}]\ \ [E_{HL}]V_{HL} \\ & - k_{t,[ADB]}[ADB_{HL}][E_{HL}]V_{HL} \\ & - k_t[E_{HL}]\sum_{i=z}^{jcr-1}[P^i_{HL}]V_{HL} - V_{oil}\int_{r_{nuc}}^{r_{max}} k_{dM,HL} f(r,t)\,dr \\ & - V_{oil}\int_{r_{nuc}}^{r_{max}}\rho^E_1 f(r,t)\,dr\end{aligned} \tag{22}$$

$$\begin{aligned}\frac{d([AHB^*_{HL}]V_{HL})}{dt} = {} & k_{tr,[AHB]}[AHB_{HL}]\left(\sum_{i=z}^{j_{cr}-1}[P^i_{HL}]\right)V_{HL} \\ & - k^p_{AHB}[M_{HL}][AHB^*_{HL}]V_{HL} \\ & - k_{t,[AHB]}[AHB^*_{HL}]\left(\left(\sum_{i=z}^{j_{cr}-1}[P^i_{HL}]\right)+[E_{HL}]\right)V_{HL}\end{aligned} \tag{23}$$

$$\begin{aligned}\frac{d\left([(AHB-jM)^*_{HL}]V_{HL}\right)}{dt} = {} & k^p_{AHB}[M_{HL}][\left(AHB-(j-1)M\right)^*_{HL}]V_{HL} \\ & - k^p_{AHB}[M_{HL}][(AHB-jM)^*_{HL}]V_{HL} \\ & - k_{t,[AHB]}[(AHB-jM)^*_{HL}]\left(\left(\sum_{i=z}^{j_{cr}-1}[P^i_{HL}]\right)+[E_{HL}]\right)V_{HL}, \\ & j = 1, 2, \ldots, j_{cr}-1\end{aligned} \tag{24}$$

where k_{dM} is the desorption coefficient of a monomeric radical from the particle into the hairy layer. Similar to eqs. (23) and (24), the mass balance of the surfactant radicals $[((AHB-jM)^*_o,\ j=0,1,\ldots,j_{cr}-1)]$ in the oil phase can be obtained.

In eqs. (7) and (21), ρ^E_0 and ρ^0_{init} are the overall rate coefficient entries of the monomeric and initiator-derived oligomers from oil phase into the hairy layer, respectively, and are defined as follows:[12]

$$\rho^E_0 = 4\pi(r_s+\delta)N_{av}D_{oil}[P^0_o] \tag{25}$$

$$\rho^0_{init} \approx \frac{2f_{in}k_i[I]N_{av}}{N_p}\left\{\frac{2\sqrt{f_{in}k_i[I]k_t}}{k_p[M_o]}+1\right\}^{1-z} \tag{26}$$

where N_p is the total number of particles. The mass balance for the monomer is given by

$$\frac{dM}{dt}=-\left\{\left(\sum_{n=1}^{j_{cr}-1}(k_p+k_{tr,M})[P_o^n]\right)[M_o]+k_p[M_o][P_o^0]\right.$$
$$\left.+k_d[M_o][R_{io}]+\sum_{i=0}^{j_{cr}-1}k^p_{[AHB]}[(AHB-iM)^*_o][M_o]\right\}V_{oil}$$
$$-\sum_{j=0}^{j_{cr}-1}\left(k^p_{[AHB]}[(AHB-jM)^*_{HL}][M_{HL}]\right)V_{HL}$$
$$-\sum_{i=z}^{j_{cr}-1}k_p[M_{HL}]([P^i_{HL}]+[E_{HL}])V_{HL}$$
$$-V_{oil}\int_{r_{nuc}}^{r_{max}}\left((k_p+k_{tr,M})f_1^p+k_pf_1^M\right)[M_p]dr \quad (27)$$

where T is the total concentration of oligomers in the oil phase, defined as follows:

$$[T]=\sum_{i=0}^{j_{cr}-1}[P_o^i]+[R_{io}] \quad (28)$$

In eq. (19), V_{HL} is the total volume of the hairy layer with a length of δ around the particles, which is given by

$$V_{HL}=4\pi\delta N_{av}V_{oil}\int_{r_{nuc}}^{r_{max}}r^2f(r,t)dr \quad (29)$$

Population Balance Equations (PBEs)

The zero–one model was used to obtain the PSD. In this model, it is assumed that particles can have only one radical or no radical. The PBEs based on the zero–one kinetic model distinguish particles that have a polymeric radical (f_1^P), particles that have no radicals (f_0), and particles that have a monomeric radical (f_1^M).[23] Particles are assumed to be able to coagulate with each other.

By considering the reaction of electrosteric surfactant in the hairy layer with exiting or entry radicals in the particle, one can determine the PBEs for three types of particles (f_1^P, f_1^M and f_0) as follows:[23]

$$\frac{\partial f_0(r,t)}{\partial t}=\rho_r(f_1^p+f_1^M-f_0)+k_{dM,HL}f_1^M$$
$$+P_{des}(k_{t,[ADB]}[ADB_{HL}]f_1^M+k_{tr,[AHB]}[AHB_{HL}]f_1^M)$$
$$-f_0(r)\int_{r_{nuc}}^{r_{max}}\beta(r,r')[f_0(r')+f_1^p(r')]dr'$$
$$+\int_{r_{nuc}}^{r/2^{1/3}}\beta(r',r'')[f_0(r')f_0(r'')$$
$$+f_1^p(r')f_1^p(r'')]\frac{r^2}{(r^3-(r')^3)^{2/3}}dr' \quad (30)$$

$$\frac{\partial f_1^p(r,t)}{\partial t}=\rho_{init}f_0-\rho_rf_1^p-k_{tr,M}[M_p]f_1^p+k_p[M_p]f_1^M$$
$$-\frac{\partial\left((dr/dt)f_1^p(r)\right)}{\partial r}+R_{nuc}\underline{\delta}\ (r-r_{nuc})$$
$$-f_1^p(r)\int_{r_{nuc}}^{r_{max}}\beta(r,r')[f_0(r')$$
$$+f_1^p(r')]dr'+\int_{r_{nuc}}^{r/2^{1/3}}\beta(r',r'')[f_0(r')f_1^p(r'')$$
$$+f_0(r'')f_1^p(r')]\frac{r^2}{(r^3-(r')^3)^{2/3}}dr' \quad (31)$$

$$\frac{\partial f_1^M(r,t)}{\partial t}=k_{tr,M}[M_p]f_1^p(r)-(k_p\ [M_p]\ +\rho_r$$
$$+k_{dM,HL}\ )f_1^M(r)+\rho_I^Ef_0(r)-P_{des}(k_{t,[ADB]}[ADB_{HL}]f_1^M$$
$$+k_{tr,[AHB]}[AHB_{HL}]f_1^M) \quad (32)$$
$$f(r,t)=f_1^p(r,t)+f_1^M(r,t)+f_0(r,t) \quad (33)$$

where the third term in eq. (30) is due to the influence of the electrosteric surfactant,[23] and the other terms in the previous equations are common terms used in electrostatic systems. r' and r'' are related by the volume additivity condition:$(r'')^3+(r')^3=(r)^3$. It should be noted that the coagulation of particles containing monomeric radicals is neglected because the number of this type of particles was low relative to particles containing polymeric radicals or no radicals. In eq. (31), $\underline{\delta}$ denotes the Dirac function.

Changes in the total number of particles can be obtained by the integration of f given in eq. (33) over the whole range of particles sizes. Similarly, variations in the total numbers of polymeric radicals, particles that have no radicals, and particles that have a monomeric radical can be obtained by the integration of their corresponding density functions (f_1^P),(f_0), and (f_1^M) over the whole range of particles sizes.

$$P_{des}=\frac{k_{dM}}{(k_{dM}+k_p\ [M_p])} \quad (34)$$

In the eq. (30), P_{des} is the probability of a monomeric radical that exits from the particle interior and enters the hairy layer and is defined as follows: where k_{dM} is the desorption coefficient of a monomeric radical from the particle into the hairy layer.[8,9] In the eq. (30), $k_{dM,HL}$ is the rate coefficient for complete desorption of a monomeric radical into the oil phase through the hairy layer with consideration of the reaction in the hairy layer. The desorption of a monomeric radical into the oil phase through the hairy layer in the absence of a reaction in the hairy layer ($k'_{dM,HL}$) is as follows:[25]

$$k'_{dM,HL}\ =\frac{\lambda\gamma N_{av}}{\eta m}\left(1-\frac{\lambda N_p}{\lambda N_p+k_p\ [M_o]+2k_t[P_o^0]}\right) \quad (35)$$

where

$$\eta=\frac{k_p\ [M_p]}{D_p},\quad \gamma=\frac{\left(\frac{k_{tr,M}\ [M_p]}{V_sN_{av}}\right)}{D_p},$$
$$\lambda=\frac{4\pi D_{oil}r_s}{1+\frac{D_{oil}}{D_h}\ \frac{\delta}{r_s}+\frac{D_{oil}}{D_pm}\ \frac{1}{r_s\sqrt{\eta}}\ \coth(r_s\sqrt{\eta})-1} \quad (36)$$

where m is the ratio of the monomeric radical concentration in the particle phase to its concentration in the hairy layer. The concentration of the monomeric radical in the hairy layer is calculated with eq. (22). The concentration of the monomeric radical in the particle phase is obtained from the following equation:

$$[E]=\frac{\int_{r_{nuc}}^{r_{max}}f_1^M(r,t)dr}{N_{av}\int_{r_{nuc}}^{r_{max}}\frac{4}{3}\pi r^3f_1^M(r,t)dr} \quad (37)$$

To consider the effect of the reaction of the exiting monomeric radical in the hairy layer on the $k'_{dM,HL}$, it is multiplied by $P^{[E]}_{exit}$.

This shows the probability of the desorption of the monomeric radical through the hairy layer into the oil phase. This probability is given by the following equation:

$$P_{exit}^{[E]} = \frac{k'_{dM,\mathrm{HL}}}{[\mathrm{k_{t,[ADB]}}][\mathrm{ADB_{HL}}][E_{\mathrm{HL}}]N_{\mathrm{av}}V_{\mathrm{HL}} + k'_{dM,\mathrm{HL}}]} \quad (38)$$

The rate coefficient for the complete desorption of a monomeric radical into the oil phase through the hairy layer with consideration of the reaction in the hairy layer ($k_{dM,\mathrm{HL}}$) is as follows:

$$k_{dM,\mathrm{HL}} = P_{exit}^{[E]}\ k'_{dM,\mathrm{HL}} \quad (39)$$

In eq. (31), R_{nuc} and $\frac{dr}{dt}$ are the nucleation and growth rates of the particle, respectively. The nucleation of the particles in EP and IEP occurred by micellar and homogeneous mechanisms. In IEP, micellar nucleation occurred when the free surfactant concentration in the oil phase exceeded the critical micelle concentration (cmc). Above cmc, the excess surfactant molecules aggregate in the continuous phase (oil), and micelles are produced. The concentration of these micelles is given by[24,26]

$$C_{Micelle} = \max\left(\frac{\frac{S_{\mathrm{oil}}}{V_{\mathrm{oil}}} - CMC}{n_{agg}},\ 0\right) \quad (40)$$

where n_{agg} is the aggregation micellar number. When the length of oligomeric radicals reaches the critical length of z, they can enter the micelles and produce polymer particles by propagation reaction. The rate of micellar nucleation is given by[24]

$$R_{Micellar} = \sum_{i=z}^{j_{cr}-1} \rho_{\mathrm{init}}^{i} C_{Micelle} \quad (41)$$

The oligomeric radicals with a chain length of j_{cr} can produce polymeric particles. The rate of homogeneous nucleation is given by[24]

$$R_{Homogenous} = k_p[P_o^{j_{cr}-1}][M_o] \quad (42)$$

The total rate of nucleation is obtained by

$$R_{\mathrm{nuc}} = R_{Micellar} + R_{Homogenous} \quad (43)$$

The particle growth rate is obtained from the following equation:[26]

$$\frac{dr}{dt} = \frac{1}{4\pi r^2 \rho_p N_{\mathrm{av}}} k_p[M_p]M_w \quad (44)$$

where p_p is the average density of produced polymer. According to the investigation of Capek[13] and Thickett and Gilbert,[16] it is obvious that radical entry rate into the particle decreases because of the reaction of the entry radical with the electrosteric surfactant. Therefore, the modified version of the entry model "oil phase growth control" can be obtained by the incorporation of the transfer and termination reactions of the surfactant with radicals in the system. The reactions with the surfactant in the hairy layer for an entry radical can be easily added to the conventional equations, and the modified expression for ρ_{init} is given as follows:[25]

$$\rho_{\mathrm{init}} \approx \frac{2f_{in}k_i[I]N_{\mathrm{av}}}{N_p}\left\{\frac{2\sqrt{f_{in}k_i[I]k_t} + (\mathrm{k_{t,[ADB]}}[\mathrm{ADB_{HL}}] + k_{\mathrm{tr,[AHB]}}[\mathrm{AHB_{HL}}])}{k_p[M_o]} + 1\right\}^{1-z} \quad (45)$$

Assuming that the exiting monomeric radical in the oil phase can reenter the original particle or another one, the reentry rate coefficient (ρ_{Io}) for the monomeric radical is defined by the Smoluchowski expression for a diffusion-controlled reaction for electrostatic surfactants. Because of the resistance of the hairy layer against the diffusion of monomeric radicals into the particle due to the steric barrier of the electrosteric surfactant around the PAM particles (ρ_{I0}), similar to the studies of Crowley *et al.*[17] and Zeaiter *et al.*[26] and with the assumption of no reaction in the hairy layer, has been modified as given next:

$$\rho_{I0} = 4\pi r_s N_{\mathrm{av}} D_{eq}[P_o^0] \quad (46)$$

where D_{eq} is the equivalent diffusion coefficient of the monomeric radical from oil and hairy layer phases into the particle and can be obtained from the following equation:

$$D_{eq} = \frac{\left(1 + \frac{\delta}{r_s}\right)D_{\mathrm{oil}}}{\left(1 + \frac{\delta D_{\mathrm{oil}}}{r_s D_h}\right)} \quad (47)$$

where D_{oil} and D_{h} are the Diffusion coefficient of the radical in the oil phase and hairy layer around the particles, respectively. The probability of the termination reaction of entry monomeric radicals in the hairy layer by [ADB] must be considered in the radical entry rate into the particles in eq. (46). If $P_{entry}^{[E]}$ denotes the probability of entry of the monomeric radical into the particle from the hairy layer, it can be obtained from the following equation:

$$P_{entry}^{[E]} = \frac{\rho_{I0}}{[\mathrm{k_{t,[ADB]}}][\mathrm{ADB_{HL}}][E_{\mathrm{HL}}]N_{\mathrm{av}}V_{\mathrm{HL}} + \rho_{I0}]} \quad (48)$$

Therefore, by considering the reaction of entry monomeric radicals in the hairy layer, the entry rate of monomeric radicals into the particle is given by

$$\rho_I^E = P_{entry}^{[E]}\ \rho_{I0} \quad (49)$$

Overall, the rate of radical entry (ρ_r) is obtained as[9,17]

$$\rho_r = \rho_{rp}^i = \rho_{rm}^i = \rho_{\mathrm{init}}^i + \rho_I^E = \rho_{\mathrm{init}} + \rho_I^E \quad (50)$$

where ρ_{rp}^i and ρ_{rm}^i are the entry radical coefficients of an oligomer with i monomer into a particle and a micelle with radius r, respectively.

Average MW

According to the investigation of Clay and Gilbert[27] and because of the radical transfer and termination by the surfactant molecules in the hairy layer, MW distribution can be obtained as follows:

$$\frac{d\bar{P}(\bar{M})}{dt}=\left(\rho_r+k_{tr,M}[M_p]+P_{des}(k_{t,[ADB]}[ADB_{HL}]\ +k_{tr,[AHB]}[AHB_{HL}])\right)$$
$$\times\bar{n}\exp\left(\frac{-\left(\rho_r+k_{tr,M}[M_p]+P_{des}(k_{t,[ADB]}[ADB_{HL}]+k_{tr,[AHB]}[AHB_{HL}])\right)}{k_p[M_p]}\ \frac{\bar{M}}{M_w}\right) \quad (51)$$

where $\bar{P}(\bar{M})$ is the total number of dead chains with a molecular weight of $\bar{M}$. The number-average and weight-average molecular weights (M_n and M_w, respectively) are given by

$$\langle M_n\rangle=\frac{\int_1^\infty \bar{M}\ \bar{P}(\bar{M})d\bar{M}}{\int_1^\infty \bar{P}(\bar{M})d\bar{M}} \quad (52)$$

$$\langle M_w\rangle=\frac{\int_1^\infty \bar{M}^2\ \bar{P}(\bar{M})d\bar{M}}{\int_1^\infty \bar{M}\ \bar{P}(\bar{M})d\bar{M}} \quad (53)$$

COAGULATION MODELING

Coagulation can affect the PSD and stability of the particles. Ignoring this phenomenon in some cases can lead to modeling error. In this section, the coagulation mechanism and coagulation rate are discussed.

Coagulation Mechanisms

Two different mechanisms may lead to particle coagulation in EP and IEP: perikinetic aggregation (because of Brawnian motion) and shear or orthokinetic aggregation (because of transport by fluid motion). The contributions of these two mechanisms to the overall coagulation rate are not necessarily additive and depend on the polymerization recipe, mixing rate, particle size, shear rate, and colloidal stability.[28]

To relate the particle surface charge to the perikinetic aggregation, the classical DLVO model, which accounts for the electrostatic repulsive potentials (U_R) and the van der Waal's attractive potentials (U_A), are used. However, a large number of studies have indicated that in many colloidal systems, additional short-range repulsive forces, which decay exponentially with distance, are often present.[18,19] Indeed, although the classical DLVO theory remains the basic approach for the stability of EP or IEP systems, this theory has been found to be unable to fully describe all of the static and dynamic behaviors. Common examples of the non-DLVO forces are structural forces due to the concentration of water molecules in hydration shells and the steric hindrance force of surfactant.[19,29] Different methods have been proposed in the literature to account for this short-range repulsive interaction to explain the experimental results.[18,29] However, there are still few parameters in these models that cannot be evaluated accurately either experimentally or theoretically. Moreover, this short-range repulsive force can be different in different systems, and a model developed for a specific colloidal system is often difficult to apply to other systems.[18,29] Thus, for the considered system, in addition to the DLVO interactions, the non-DLVO interactions due to the hydration force of high electronegative atoms in the amine groups of the polymer chains and the steric force due to the use of the electrosteric surfactant (Span 80) were also taken into account.

Coagulation Rate

The coagulation rate coefficient (β) between particles of swollen radii r_s, and r_s' was obtained from the Fuchs' modified Smoluchowski equation for perikinetic aggregation:[24,28]

$$\beta(r_s,r_s')=\frac{2k_BT}{3\mu\omega(r_s,r_s')}\left(2+\frac{r_s}{r_s'}+\frac{r_s'}{r_s}\right) \quad (54)$$

where μ is the viscosity of the continuous phase and ω is the Fuchs' stability ratio. The stability ratio is the inverse of the collision efficiency and accounts for the presence of colloidal and hydrodynamic interactions between the particles. Theories of coagulation start with diffusion in a potential and/or flow field, as described by the appropriate conservation equation. It is assumed that any particle that goes over the repulsive barrier between the particles (through shear and/or Brownian motion) undergoes irreversible coagulation. The Fuchs' stability ratio for binary collisions can be obtained by the following equation:[28]

$$\omega=(r_s+r_s')\int_{r_s+r_s'}^{\infty}\exp\left(\frac{U(r)-G.(r_s+r_s')^4/r}{k_BT}\right)\frac{dr}{r^2} \quad (55)$$

where k_B is the Boltzman constant, T is the absolute temperature, U is the total particle interaction energy and G is the hydrodynamic interaction function. A useful rule of thumb can be established by the computation of the quotient of the rate coefficients derived for the limiting cases of pure perikinetic and orthokinetic aggregation of two noninteracting particles.[28] Orthokinetic aggregation is favored by high shear rates and large particle sizes. Therefore, for a low mixing rate (600 rpm), the orthokinetic aggregation is neglected in coagulation.

The total inter particle interaction energy is given by the sum of the attractive van der Waal's forces (U_A), repulsive potentials (U_R's), and hydration interactions (U_{Hyd}) as follows:

$$U=U_A+U_R+U_{Hyd} \quad (56)$$

DLVO Forces

The attractive potential attributed to the universal van der Waal's force of attraction is given by[30]

$$U_A=-\frac{A}{6}\left[\frac{2r_sr_s'}{r^2-(r_s+r_s')^2}+\frac{2r_sr_s'}{r^2-(r_s-r_s')^2}+ln\left(\frac{r^2-(r_s+r_s')^2}{r^2-(r_s-r_s')^2}\right)\right] \quad (57)$$

where A is the Hamaker constant, which accounts for the effects of the various intrinsic (internal) interactions between the particles that result in the net attractive potential.

Table II. Parameters Used for Acrylamide Polymerization Simulation

Parameter	Value	Reference
k_i (min^{-1})	7×10^{16} exp (−139805/*RT*)	13
k_p ($dm^3\ mol^{-1}\ min^{-1}$)	9.9×10^{7} exp (−2743/*RT*)	37
$k_{tr,M}$ ($dm^3\ mol^{-1}\ min^{-1}$)	5.73×10^{8} exp (−10438/*RT*)	37
k_d ($dm^3\ mol^{-1}\ min^{-1}$)	k_p	11
k_t ($dm^3\ mol^{-1}\ min^{-1}$)	5.07×10^{11} exp (−1482/*RT*)	37
j_{cr}	133	38
z[a]	4	12
$k_{t,[ADB]}$ ($dm^3\ mol^{-1}\ min^{-1}$)[b]	$2.54\times10^{-2}k_t$	11
$k_{tr,[AHB]}$ ($dm^3\ mol^{-1}\ min^{-1}$)	$7.55\times10^{-8}\exp(1455/T)/(\Gamma\ r_s)$	11
$k^p_{[AHB]}$ ($dm^3 mol^{-1} min^{-1}$)	k_p	11
$k^t_{[AHB]}$ ($dm^3 mol^{-1} min^{-1}$)	k_t	11
K_{po}	1/7000	12
a_{ed} (A^2)	69	11
f_{in}	0.5	13
cmc_{Span80} (mol/L)	1.7×10^{-5}	39
n_{agg}	120	39
D_p (cm^2/s)	2.933×10^{-12}	40
D_{oil} (cm^2/s)	4.2×10^{-9}	40
$\Gamma\infty=1/a_s\ N_{av}$ (mol/m^2)	2.4×10^{-6}	11
a_s (A^2)	69	11
$\delta = L$ (nm)	2.2	11
D_h (cm^2/s)	$0.143D_{oil}$	This study
c_1	2.61	This study
δ_H (nm)	0.48	This study
F_0^H(N m^{-2})	5.37×10^{7}	This study

[a] In the cited reference, *z* was equal to 3.6 and was rounded to 4.
[b] Calculated with the data given in the cited reference

The repulsive electrostatic and steric potentials between two particles (U_R) depend on type of the surfactant. In the case of the nonionic (electrosteric) surfactants, such as Span 80, the electrostatic repulsive potential is equal to zero.

Non-DLVO Forces

Unlike electrostatic surfactants, the repulsive potential for the nonionic (electrosteric) surfactants is due to the steric hindrance of the surfactant tail. Therefore, this repulsive potential, including the non-DLVO forces, is as follows:[31]

$$U_R = c_1 \frac{2r_s r_s'}{r_s + r_s'} \cdot \frac{100L^2}{\pi} \Gamma^{2/3} k_B T e^{-\pi r/L} \tag{58}$$

where L is the thickness of the surfactant layer, Γ is the surfactant coverage on the particle, and c_1 is an adjustable constant. It should be noted that in the previous equation, L is equal to the thickness of the hairy layer. The surfactant coverage on the particle can be obtained through the following equation:[11]

$$\Gamma = \frac{\theta}{a_s N_{av}} = \Gamma_\infty \theta \tag{59}$$

where a_s is the area occupied by a single molecule of surfactant, and Γ_∞ is the saturated surfactant surface coverage. The PAM particle surface will be hydrated because of the adsorption of water molecules to the particle surface by hydrogen bonding between the amine groups of PAM and water molecules. Therefore, for coagulation between the PAM particles, an additional force is required for the dehydration of the particle surface and the removal of water molecules. To calculate U_{Hyd}, an exponential decay function is used to describe the hydration force between particles (F_{Hyd}) as given next:[32,33]

$$F_{Hyd} = F_0^H \exp\left(\frac{-h}{\delta_H}\right) \tag{60}$$

where $h = r - (r_s + r_s')$ is the surface-to-surface distance between particles, F_0^H is the hydration force constant, and δ_H is the characteristic decay length. The corresponding hydration interaction energy between two spherical particles with radii r_s and r_s' can be obtained by the integration of eq. (60) and the Derjaguin approximation:[34]

$$U_{Hyd} = \int_{r-(r_s+r_s^1 r_s')}^{\infty} \pi \frac{2r_s r_s'}{r_s + r_s'} F_0^H \delta_H \exp\left(\frac{-h}{\delta_H}\right) dh = 2\pi \frac{r_s r_s'}{r_s + r_s'} F_0^H \delta_H{}^2 \exp\left(-\frac{r-(r_s+r_s' r_s^1)}{\delta_H}\right) \tag{61}$$

where δ_H and F_0^H are unknown parameters and have been adjusted to match the experimental results as discussed in the next sections.

RESULTS AND DISCUSSION

To simulate the IEP dynamics, the mass and PBEs must be solved simultaneously by an appropriate method. In this study, the moment method with an order of eight was used to solve the PBEs.[35] To obtain the PSD from its moments, the maximum entropy approach was used.[36]

In the suggested model, some parameters, such as D_h, c_1, F_0^H and δ_H are undetermined and should be fixed. For this purpose, the experimental results obtained under the conditions explained in the Experimental section (the nominal case) and the following performance index were used to determine the previous parameters:

$$PI = \sum_{i=1}^{n_s} \left(\frac{MW_{exp}(i) - MW_{model}(i)}{MW_{exp}(i)} \right)^2 + \left(\frac{d_{exp}(i) - d_{model}(i)}{d_{exp}} \right)^2 \quad (62)$$

where n_s is the number of samples taken during the reaction time. Because the average MW and average number particle size are the most important product specifications, only these properties were considered in the previous performance index. The values of c_1, F_0^H and δ_H obtained from the previous procedure were in the ranges reported in the literature.[31,32] The value of D_h should be between its values in the organic and particle phases. Again, the obtained value for this parameter was in this range. The values of the tuning parameters were obtained on the basis of the experimental data for the nominal case (surfactant concentration = 0.002 mol/L) and were fixed to predict the polymer properties under different experimental conditions to validate the obtained model. In the numerical simulation, we assumed that r_{max} and r_{nuc} were 400 and 22 nm, respectively. The other parameters used in the simulation study are given in Table II.

To verify the effects of different forces on the final specifications of the produced polymer, we conducted different simulations for the nominal case by neglecting coagulation or hydration and steric forces in coagulation modeling. The results are shown in Figure 3. As shown in Figure 3(a), neglecting the coagulation effect resulted in a narrower distribution and shifted the PSD toward the smaller sizes. Neglecting the hydration or steric forces, which were repulsive, increased the coagulation effect; therefore, the final PSD became wider and shifted toward larger particle sizes. Coagulation had similar effects on the monomer conversion and the average MW. As shown in Figure 3(b), coagulation reduced the monomer conversion because the coagulation of particles containing radicals produced a particle with no radical because of the termination effect. Decreasing the number of particles that contained radicals, in turn, resulted in a lower conversion. Neglecting the hydration or steric forces increased the coagulation rate, and this led to a lower conversion. Figure 3(c) shows the effect of coagulation on the average MW. Coagulation increased the average MW because the polymeric chains could become longer not only by propagation but also because of particle coagulation. Similarly, neglecting the hydration or steric forces, which increased the coagulation rate, led to an increase in the average MW. Figure 3 indicates that the steric force had a slightly stronger effect on the polymer final specifications with respect to the hydration force. As shown in Figure 3, when all of the forces were considered in the coagulation modeling, less deviation from the experimental data was observed.

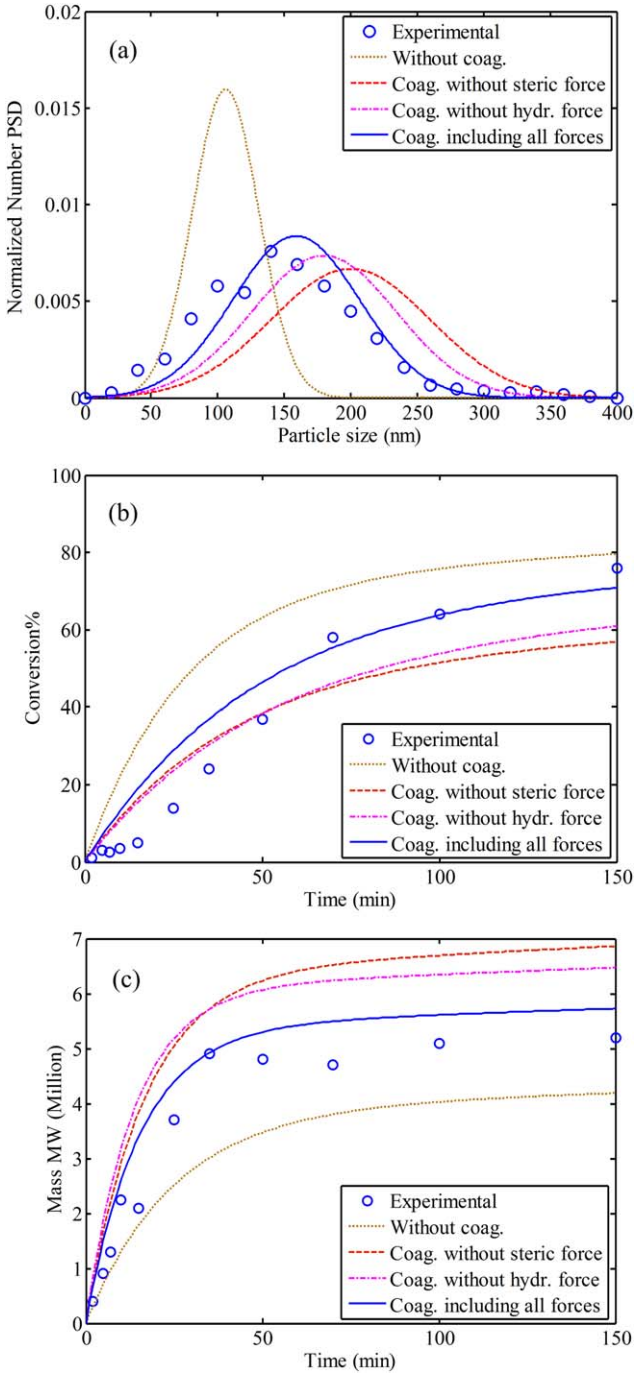

Figure 3. Effects of different forces in coagulation modeling with fixed adjustable parameters on the (a) final PSD, (b) monomer conversion, and (c) average MW. [Color figure can be viewed in the online issue, which is available at wileyonlinelibrary.com.]

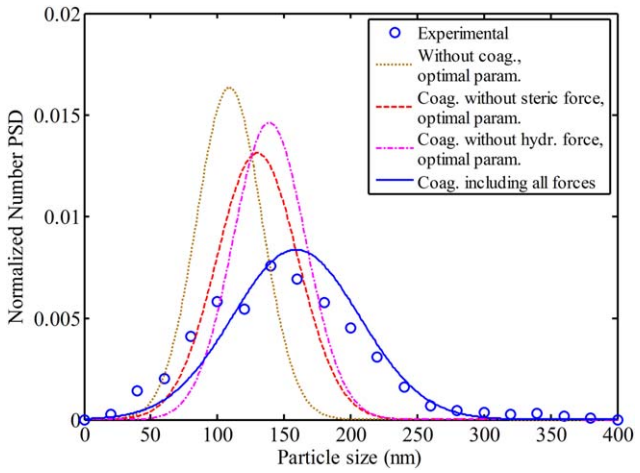

Figure 4. Effects of different forces on the final PSD in coagulation modeling with optimal adjustable parameters. [Color figure can be viewed in the online issue, which is available at wileyonlinelibrary.com.]

When the adjustable parameters for each case were optimized on the basis of the objective function [eq. (62)], the final PSDs were found, as shown in Figure 4. As shown, again, the best result belonged to the case where all forces were taken into account in coagulation modeling.

Similar results were obtained for conversion and MW (not shown).

The experimental and simulation results concerning the effect of the surfactant concentration on the conversion and average MW of produced PAM are shown in Figure 5. In these experiments, the concentration of surfactant was changed (to 0.002, 0.01, and 0.02 mol/L) to verify the effect of the surfactant concentration. As shown, there was relatively good agreement between the simulation results and the experimental data.

As shown in Figure 5(a), with increasing surfactant concentration, the average MW first decreased and then increased. This behavior could be explained as follows. Increasing the surfactant concentration had two effects. The first effect was the increase of the number of micelles, and the second one was the increase in the reaction of active radicals with surfactant molecules around the particles; this resulted in the reduction in the concentration of active radicals, which could participate in the propagation reaction. Because of the first effect, the total radical entry rate into the growing particles increased, and this led to an increase in the termination rate, which resulted in a lower average MW. When the surfactant concentration was increased above a certain level (0.01 mol/L), the second effect became dominant, and the concentration of active radicals decreased because of their reaction with surfactant molecules; this led to a decrease in the termination rate. This, in turn, resulted in a higher average MW. Variations of the monomer conversion with changing surfactant concentration [Figure 5(b)] could be explained as follows. When the number of micelles was increased, the number of growing particles increased, and this resulted in an increase in the initial rate of conversion, and when the surfactant concentration exceeded a certain level, the second effect became dominant, which led to a reduction in the conversion. As shown in Figure 5, there was good agreement between the simulation results the experimental data.

The effects of the surfactant concentration on the number-average particle size and final PSD are shown in Figure 6. As shown, when the surfactant concentration was increased, the final PSD became narrower and shifted to the smaller size [Figure 6(a)], and the average particle size decreased [Figure 6(b)]. This behavior could be explained as follows. The increase in the initial amount of surfactant led to an increase in the particle number because of the increase in the nucleation rate. When the surfactant concentration was increased, the particles became more stable, and this led to a decrease in the coagulation rate and a shift of the PSD toward the smaller particle sizes. This effect, in turn, resulted in a narrower final PSD. As shown, there was good agreement between the simulation results and the PSD experimental data.

Figure 7(a,b) shows the effect of the initiator concentration on the monomer conversion and the average MW, respectively. When the concentration of the initiator was increased, the number of radicals increased, and therefore, propagation was carried

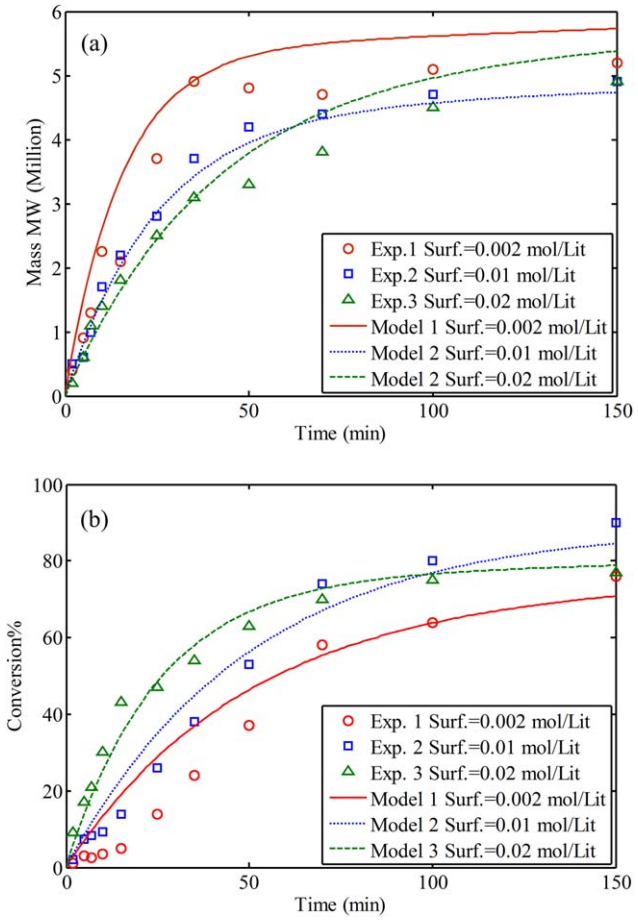

Figure 5. Effect of the surfactant concentration on the (a) M_w of the polymer and (b) monomer conversion. [Color figure can be viewed in the online issue, which is available at wileyonlinelibrary.com.]

out in more micelles simultaneously. The increase in the total rate of propagation resulted in an increase in the monomer conversion. The increase in the initiator concentration also led to the increase in the number of oligomeric radicals; this, in turn, increased the termination rate and decreased the average MW.

CONCLUSIONS

In this study, the zero–one model was used to model the IEP of acrylamide in a batch reactor to predict the conversion, average MW, and PSD of the PAM product. In the PBE, the effect of coagulation was included. Because of the high electronegativity of oxygen and nitrogen atoms in the chemical amine groups of the PAM particles, the presence of water molecules, and also the steric hindrance of the surfactant, not only the DLVO forces but also the hydration and steric forces should be considered in coagulation modeling. In the modeling of IEP, the effect of the surfactant, the steric barrier of the electrosteric surfactant (Span 80), and its reaction with radicals, including monomeric radicals, on the radical entry rate into the particle were taken into account. The model was validated by a comparison of the simulation results with experimental data, and good agreement was observed. The effects of different forces on the coagulation rate were investigated by a comparison of the experimental data and the simulation results. The results indicate that when coagulation with all of the forces, including DLVO, hydration, and steric forces, was considered, it had a better performance compared to cases where some of these forces were neglected. The effects of the surfactant and initiator concentrations on the final polymer properties were investigated by simulation and experimental studies. It was shown that the model could predict these effects fairly well. The results indicate that when the surfactant concentration was increased above a certain level, because of the reactions of radicals with surfactant molecules and the surfactant steric hindrance effect, the number-average particle size and monomer conversion decreased, and the final average MW increased. The increase in the initiator concentration led to an increase in the monomer conversion and a decrease in the average MW.

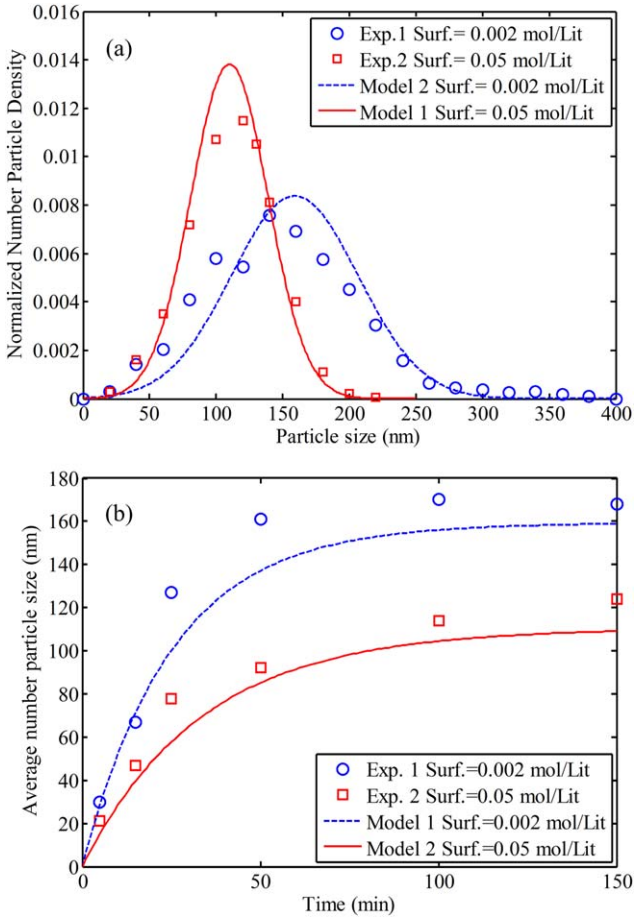

Figure 6. Effect of the surfactant concentration on the (a) final PSD and (b) average particle size. [Color figure can be viewed in the online issue, which is available at wileyonlinelibrary.com.]

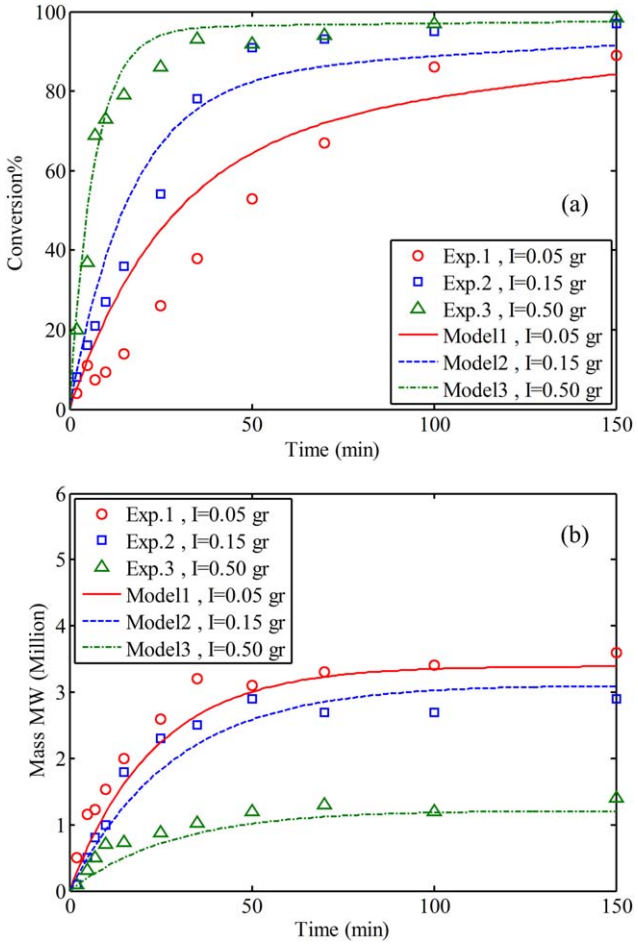

Figure 7. Effect of the initiator concentration on the (a) monomer conversion and (b) mass MW of the polymer. [Color figure can be viewed in the online issue, which is available at wileyonlinelibrary.com.]

REFERENCES

1. Taylor, K. C.; Nasr-El-Din, H. A. *J. Petrol. Sci. Eng.* **1998**, *19*, 265.
2. Graillat, C.; Pichot, C.; Guyot, A.; El-Aasser, M. S. *J. Polym. Sci. Part A: Polym. Chem.* **1986**, *24*, 427.

3. Vanderhoff, J. W.; Distefano, F. V.; El-Aasser, M. S.; O'Leary, R.; Shafer, O. M.; Visioli, D. L. *J. Dispersion Sci. Technol.* **1984**, *5*, 323.
4. Vanderhoff, J. W.; Bradford, E. B.; Tarkowski, H. L.; Shaffer, J. B.; Wiley, R. M. *Adv. Chem. Ser.* **1962**, *34*, 32.
5. Barari, M.; Abdollahi, M.; Hemmati, M. *Iran. Polym. J.* **2011**, *20*, 65.
6. Chen, L. W.; Yang, W. J. *Polym. Sci. Part A: Polym. Chem.* **2004**, *42*, 846.
7. Schulz, D. N. In Water-Soluble Polymers: Synthesis, Solution, Properties and Applications; Shalaby, W., Ed.; ACS Symposium Series 467; American Chemical Society: Washington, DC, **1991**; p 93.
8. Coen, E. M.; Peach, S.; Morrison, B. R.; Gilbert, R. G. *Polymer* **2004**, *45*, 3595.
9. Gilbert, R. G. Emulsion Polymerization: A Mechanistic Approach; Academic: London, **1995**.
10. Odian, G. Principles of Polymerization, 4th ed.; Wiley: New York, **2004**; p 171.
11. Hunkeler, D.; Hamielec, A. E.; Baade, W. *Polymer* **1989**, *30*, 127.
12. Alexander, P.; Kristina, P.; Karl-Heinz, R. *Polym. Int.* **1998**, *45*, 229.
13. Capek, I. *Polym. J.* **2004**, *36*, 793.
14. Niranjan, P. S.; Tiwari, A. K.; Upadhyay, S. K. *J. Appl. Polym. Sci.* **2011**, *122*, 981.
15. Omidian, H.; Zohuriaan-Mehr, M. J.; Bouhendi, H. *Eur. Polym. J.* **2003**, *39*, 1013.
16. Thickett, S. C.; Gilbert, R. G. *Macromolecules* **2006**, *39*, 6495.
17. Crowley, T. J.; Meadows, E. S.; Kostouas, E.; Doyle, F., III *J. Process Control* **2000**, *10*, 419.
18. Boström, M.; Deniz, V.; Franks, G. V.; Ninham, B. W. *Adv. Colloid Interface Sci.* **2006**, *123*, 5.
19. Molina-Bolivar, J. A.; Galisteo-Gonzalez, F.; Hidalgo-Alvarez, R. *Colloids Surf. B* **1999**, *14*, 3.
20. Ramazani, A. S. A.; Nourani, M.; Emadi, M. A. *Iran. Polym. J.* **2010**, *19*, 53.
21. Alexander, P.; Kristina, P.; Karl-Heinz, R. *Polym. Int.* **1998**, *45*, 22.
22. Alb, A. M.; Farinato, R.; Calbick, J.; Reed, W. F. *Langmuir* **2006**, *22*, 831.
23. Thickett, S. C.; Marianne, G.; Gilbert, R. G. *Macromolecules* **2007**, *40*, 4710.
24. Immanuel, C. D.; Cordeiro, C. F.; Sandaram, S. S.; Meadows, E. S.; Crowley, T. J.; Doyle, F. J., III. *Compos. Chem. Eng.* **2002**, *26*, 1133.
25. Asua, J. M. *Macromolecules* **2003**, *36*, 6245.
26. Zeaiter, J.; Romagnoli, J. A.; Barton, G. W.; Gomes, V. G.; Hawkett, B. S.; Gilbert, R. G. *Chem. Eng. Sci.* **2002**, *57*, 2955.
27. Clay, P. A.; Gilbert, R. G. *Macromolecules* **1995**, *28*, 552.
28. Elgebrandt, R. C.; Romagnoli, J. A.; Fletcher, D. F.; Gomes, V. G.; Gilbert, R. G. *Chem. Eng. Sci.* **2005**, *60*, 2005.
29. Yong, H.; Zhu, B.; Yoshio, I. *Prog. Polym. Sci.* **2004**, *29*, 1021.
30. Masliyah, J. H.; Bhattacharjee, S. Electrokinetic and Colloid Transport Phenomena, 3rd ed.; Wiley: Hoboken, NJ, **2006**; p 401.
31. Israelachvili, J. N. Intermolecular and Surface Forces, 3rd ed.; Academic: Amsterdam, **2011**; p 131.
32. Israelachvili, J. N.; Adams, G. E. *J Chem. Soc. Faraday Trans. 1* **1978**, *74*, 975.
33. Runkana, V.; Somasundaran, P.; Kapur, P. C. *AIChE J.* **2005**, *51*, 1233.
34. Derjaguin, B. V. *Kolloid* **1934**, *69*, 155.
35. Diemer, R. B.; Olson, J. H. *Chem. Eng. Sci.* **2002**, *57*, 2211.
36. Vafa, E.; Shahrokhi, M.; Abedini, H. *Chem. Eng. Commun.* **2013**, *200*, 20.
37. Currie, D. J.; Dainton, F. S.; Watt, W. S. *Polymer* **1965**, *6*, 451.
38. Fuxmana, A. M.; Mcauleya, K. B.; Schreiner, L. *J. Chem. Eng. Sci.* **2005**, *60*, 1277.
39. Leena, P. Ph.D. Thesis, University of Helsinki, **2001**.
40. Gao, J.; Penlidis, A. *Prog. Polym. Sci.* **2002**, *27*, 403.